Double Layer Effects on the Voltammetry of Self Assembled Monolayers

Michael J. Honeychurch
PO Box 23
Monash University 3800, Victoria, Australia

Abstract

When self assembled monolayers (SAMs) containing redox centres behave ideally it is a relatively straight forward process to interpret cyclic sweep voltammograms and extract thermodynamic and kinetic information. Unfortunately it is rare that the criteria for ideality are met and other models have to be developed from which to extract information. This review discusses some of the factors which influence the cyclic voltammetry of redox SAMs in particular focussing on how double layer effects influence reversible and irreversible voltammograms. The differences between Butler-Volmer kinetics and Marcus theory kinetics are also discussed.

Introduction

During the last 20 years there has been a sustained interest in the electrochemical study of adsorbed redox self assembled monolayers (SAMs). Typically the SAM is a mixture of redox and non-redox molecules. The analysis of cyclic voltammograms of redox SAMs is generally based on the methods published by Laviron in an extensive review of electrochemical methods for the study of adsorbed molecules [1]. Murray has since briefly reviewed voltammetric methods for the study of adsorbates as part of broader reviews of modified electrodes [2, 3]. When adsorbates behave "ideally" it is a relatively simple process to interpret voltammograms and extract thermodynamic and kinetic information. Unfortunately it is rare that the criteria for ideality are met and researchers then have to look to other models from which to extract information about the adsorbed redox system of interest. The models discussed in references 1-3 primarily attributed the departure from apparent non-ideal voltammetric response to the influence of lateral interactions between adsorbates. Based on additional research in this area, several other explanations of apparent non-ideal electrochemical behavior of adsorbed molecules have since been offered such as double layer effects, ion pairing, acid-base dissociation, and dispersion of formal potentials. Some of these contributing factors have recently been reviewed by Finklea as part of a review of SAMs [4] and by Honeychurch and Rechnitz [5, 6].

The purpose of this review is to discuss various models for interpreting the cyclic voltammetry (CV) of redox SAMs. Cyclic voltammetry has been the most commonly used techniques to study the equilibrium and kinetics of redox SAMs.

We will consider the reduction of a molecule, Ox, with charge z_O

$$\mathrm{Ox}^{z_O} + ne^- \Leftrightarrow \mathrm{Red}^{z_R} \qquad (1)$$

The faradaic current for the reaction of surface bound molecules is

$$i = nFA\left(k_f\Gamma_R - k_b\Gamma_O\right) \qquad (2)$$

where k_f and k_b are the forward and backward rates and Γ_O and Γ_R are the surface concentrations of oxidized and reduced molecules. The total surface concentration Γ_T, is constant during the

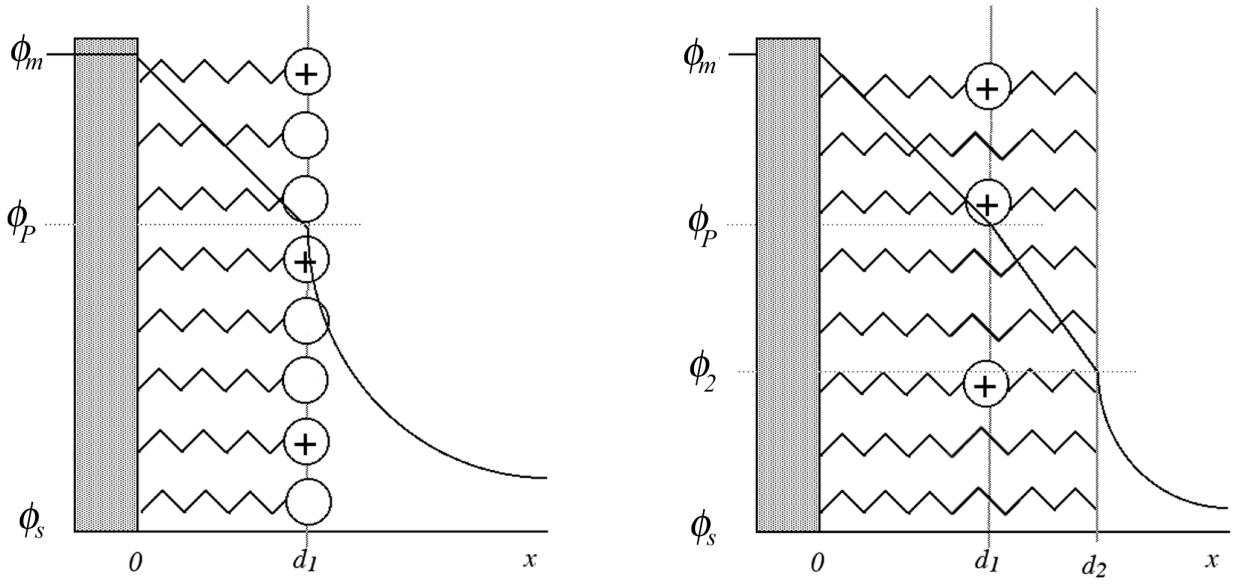

Figure 1. (a) Drawing of a SAM showing the redox centers located at the plane of electron transfer (at d_1) in contact with the solution. The potential profile in the region $0 \le x \le d_1$ which has a dielectric constant of ε_1 and capacitance C_1 is assumed to be linear. (b) Same as (a) but with the redox center located within the SAM at a distance $d_2 - d_1$ from the solution. The potential profile in the region $d_1 \le x \le d_2$ which has a dielectric constant of ε_2 and capacitance C_2 is assumed to be linear.

experiment

$$\Gamma_O(t) + \Gamma_R(t) = \Gamma_T \qquad (3)$$

Taking cathodic currents as negative the current is defined as

$$i = -nFA\frac{d\Gamma_R}{dt} \qquad (4)$$

which can be rearranged to

$$i = -nFA\Gamma_T \frac{dE}{dt}\frac{dx_R}{dE} \qquad (5)$$

where x_R, is the mole fraction of reduced molecules. In a linear sweep or cyclic voltammetric experiment the potential at any time is

$$E = E_{t=0} + \upsilon t \qquad (6)$$

where $E_{t=0}$ is the initial potential and υ is the sweep rate which is negative for a cathodic sweep and positive for an anodic sweep. It is convenient to express the current in terms of a dimensionless function; therefore after substituting $dE/dt = \upsilon$ into Eq. (5) it can be further rearranged to give

$$i = nFA\Gamma_T \upsilon\left(\frac{nF}{RT}\right)\psi \qquad (7)$$

where the dimensionless current ψ, is defined as

$$\psi = -\frac{RT}{nF}\frac{dx_R}{dE} \qquad (8)$$

Since dx_R/dE is negative for both cathodic and anodic reactions it follows that from Eq. (8) that ψ is always positive. The sign of the current is therefore governed by the sign of υ, i.e. dE/dt, which is negative for a cathodic sweep and positive for an anodic sweep.

Ideal Case

In deriving the equation for the linear sweep voltammogram it is assumed that the

entire potential drop occurs in the region $0 \leq x \leq d_1$ (figure 1) and there are no interactions between attached molecules. For the ideal case the dimensionless current is given by [1]

$$\psi = \frac{\xi}{\left(1+\xi\right)^2} \qquad (9)$$

where ξ will be used to denote the ratio of oxidized to reduced molecules.

$$\xi = \frac{\Gamma_O}{\Gamma_R} \qquad (10)$$

Under ideal conditions

$$\xi = \exp\left[\left(\frac{nF}{RT}\right)E - E_a^o\right] \qquad (11)$$

E_a^0 is the formal potential defined as

$$E_a^o = E^o + \left(\Delta G_O - \Delta G_R / nF\right) \qquad (12)$$

with ΔG being the bond energy for the covalent attachment [7]. When $\Delta G_O = \Delta G_R$ both the anodic and cathodic peaks potentials are equivalent. For $\Delta G_O \neq \Delta G_R$ a peak separation is observed. It is likely that the bond energies of the oxidized and reduced forms will not be very different from one another therefore from Eq. (12) for redox SAMs behaving ideally the formal potential of the surface reaction should be close to that of the solution reaction and the anodic and cathodic peaks potentials should be equivalent. From Eqs. (9) and (11) it can be seen that the peak will be symmetrical with ψ reaching its maximum value of 0.25 when $\xi = 1$, i.e. when $E = E_a^o$. The peak width at half peak height is $90.6/n$ mV at 25°C.

One of the problems in extracting information from experimentally obtained voltammograms is the ubiquitous peak separation that occurs even at very low sweep rates. Theory predicts that the reversible peak potential is equivalent to the formal potential and that anodic and cathodic reversible peak potentials should be identical. This is rarely observed. In cyclic voltammetry the reversible region is defined as the region, bounded on one side by $\upsilon \rightarrow 0$, in which the peak potentials are constant with increasing sweep rates, i.e. $dE_p/d\upsilon = 0$. The point at which the peak potential changes with increasing sweep rate represents the onset of quasi-reversibility. Experimental voltammograms generally exhibit some peak separation at very low sweep rates, $\Delta E_p \neq 0$, even when satisfying the criteria of reversibility, namely $dE_p/d\upsilon = 0$. Recent theories predicts an inverted Guassian shaped baseline (see below) [8] whereas a linear baseline is generally assumed when peak potentials are determined therefore a small 2-4 mV peak separation may be considered as being due to experimental uncertainties in determining the peak potential. Changes in monolayer structure and differences in solvation [9] with changes in oxidation state may also contribute to ΔE_p being non-zero. The models that have been proposed to explain the observed non-ideality are reviewed in the following sections.

As the sweep rate is increased the reaction becomes quasi-reversible and eventually irreversible. The shifting of the peak potential with increasing sweep rate that is predicted can be used to estimate the standard rate constant. The rates for the cathodic and anodic reactions are defined as

$$k_f = k_s \exp\left(-\frac{\alpha nF\eta}{RT}\right) \qquad (13)$$

$$k_b = k_s \exp\left(\left(1-\alpha\right)\frac{nF\eta}{RT}\right) \qquad (14)$$

where k_s is the heterogeneous rate constant (s^{-1}), and η is the overpotential ($\eta = E - E_a^o$). Substituting Eqs. (13) and (14) into (2) gives the Butler-Volmer equation

$$i = nFAk_s\begin{pmatrix}\Gamma_R \exp\left[\left(1-\alpha\right)nF\eta/RT\right]\\ -\Gamma_O \exp\left[-\alpha nF\eta/RT\right]\end{pmatrix} \quad (15)$$

Combining Eqs. (8)and (15) gives the general equation for the dimensionless current

$$\psi = -m\begin{pmatrix}x_R \exp\left[\left(1-\alpha\right)nF\eta/RT\right]\\ -x_O \exp\left[-\alpha nF\eta/RT\right]\end{pmatrix} \quad (16)$$

where m is a dimensionless rate constant given by

$$m = \left(RT/nF\right)\left(k_s/|\upsilon|\right) \quad (17)$$

Laviron has solved equation (16) for quasi-reversible and irreversible electron transfer [10]. As $m \rightarrow 0$ the reaction becomes totally irreversible and the solution to Eq. (16) is

$$\begin{aligned}\psi_c &= m\xi^{-\alpha}\exp\left[m\xi^{-\alpha}/\alpha\right]\\ \psi_a &= m\xi^{1-\alpha}\exp\left[-m\xi^{1-\alpha}/\left(1-\alpha\right)\right]\end{aligned} \quad (18)$$

where $\xi = \exp\left[nF\eta/RT\right]$. Equation (18) describes asymmetrical peaks with a shape that is independent of m. The peak widths at half peak height, $W_{1/2}$, of the cathodic and anodic peaks are $62.5/\alpha n$mV and $62.5/\left(1-\alpha\right)n$ respectively. As m varies the peak shifts along the potential axis. For irreversible reactions the voltammetric peak occurs when [11]

$$k^2 = \frac{dk}{dt} \quad (19)$$

where k is the forward or backward rate given by Eqs. (13) and (14).

The peak potentials are

$$\begin{aligned}E_{p_c} &= E^o_{a_c} - \left(RT/\alpha nF\right)\ln\left(\alpha/m\right)\\ E_{p_a} &= E^o_{a_a} - \left[RT/\left(1-\alpha\right)nF\right]\ln\left[\left(1-\alpha\right)/m\right]\end{aligned} \quad (20)$$

Equations (18) and (20) are approximations from a more general equation. They are valid with less than 2% error for $1/m > 12$ which occurs when $\Delta E_p > 200/n$ mV. The rate constant for the reaction can be determined after rearranging Eq. (20) to give

$$\begin{aligned}\log k_s = {} & \alpha\log\left(1-\alpha\right) + \left(1-\alpha\right)\log\alpha\\ & -\log\left(RT/nF|\upsilon|\right)\\ & -\left[\alpha\left(1-\alpha\right)nF\Delta E_p/2.3RT\right]\end{aligned} \quad (21)$$

For conditions in which $\Delta E_p < 200/n$ mV Laviron published a table from which a working curve can be constructed to determine k_s [10].

When determining the rate constant from Eq. (21) the convention seems to be to make measurements of peak separations from the mid-point $\left(E_{p_c} - E_{p_a}\right)/2$. However by measuring peak separations from the mid-point the ubiquitous peak separation obtained under reversible conditions is included in calculations of the rate constant. Equation (21) is derived assuming that $\Delta E_p = 0$ under reversible conditions and therefore peak separation is attributed solely to kinetic effects. Taking the mid point of the peak separation and defining it as a "formal potential" and substituting it into equations to determine the rate constant immediately implies that any *reversible* peak separation that exists is due to slow kinetics and is therefore contradictory. By definition if a peak separation occurs under reversible conditions it cannot be of kinetic origin. A pragmatic approach was recommended in ref. [12] in which peak separation was measured from the reversible peak potentials, $\Delta E_p = \left(E_{p_c} - E^r_c\right) - \left(E_{p_a} - E^r_a\right)$, where E^r is the reversible peak potential of the anodic and cathodic peaks. This approach has been criticized since a peak separation under reversible conditions suggests that the forward and backward reactions are not equal. Therefore the measured rate constant is not for the electron transfer but an apparent rate

constant which is possibly a composite of other rate constants. This is of course possible but if this is the case these arguments also render all other published CV methods for determining the rate constant invalid since all models assume a simple electron transfer. Alternatively, the reversible peak separation could be due to uncompensated resistance and this is discussed in more detail below.

Effect of Lateral Interactions

If interactions between molecules take place, which they may when the ratio of redox to non-redox molecules is high within the SAM, the surface activity is likely to differ from the surface concentration. Assuming that the oxidized and reduced molecules occupy the same area the activity coefficients of the adsorbates are given by Eqs. (22) and (23)

$$\gamma_O = \exp\left[-2a_{OO}\theta_O - 2a_{OR}\theta_R\right] \quad (22)$$

$$\gamma_R = \exp\left[-2a_{RR}\theta_R - 2a_{OR}\theta_O\right] \quad (23)$$

where a_{OO}, a_{RR}, and a_{OR} are the interaction coefficients, which are assumed to be independent of potential, for interactions between adsorbed O–O, R–R and O–R respectively (positive for attraction and negative for repulsion). The dimensionless current for a reversible reaction is given by [13, 14]

$$\psi = \frac{x_R\left(1 - x_R\right)}{1 - 2g\theta_T x_R\left(1 - x_R\right)} \quad (24)$$

where $g = a_{OO} + a_{RR} - 2a_{OR}$ (25)

and $\theta_T = \Gamma_T / \Gamma_m$, Γ_m is the maximum surface excess. In the context of the discussions that follow it is helpful if we substitute Eq. (10) into Eq. (24) and rearrange it to give

$$\psi = \frac{\xi}{\left(1 - \xi\right)^2 - 2g\theta_T\xi} \quad (26)$$

In Eqs. (24) and (26) the parameter g defines the shape of the peak. For $g\theta_T < 0$ the peak is smaller and broader than the ideal shape. At $g\theta_T = 2$ (strong attraction between molecules) a singularity exist which has been equated to a two dimensional phase formation. The peak width at half peak height is

$$W_{1/2} = 2\left(RT/nF\right)\left|\ln\left[\left(1+\varphi\right)/\left(1-\varphi\right)\right] - g\theta_T\right| \quad (27)$$

where $\varphi = \left[\left(2 - g\theta_T\right)/\left(4 - g\theta_T\right)\right]^{1/2}$ (28)

Laviron [13] and then later Smith et al. [15] showed that for values of $g\theta_T < 1$ a plot of $W_{1/2}$ varies linearly with $g\theta_T$ ($r = 0.9999$). Therefore for $g\theta_T < 1$, $g\theta_T$ can be determined from Eq. (29)

$$nW_{1/2} = 90.53 - 55.51g\theta_T \quad (29)$$

and the potential is given by

$$E = E_{1/2} + \left(RT/nF\right)\left[\begin{matrix} g\theta_T\left(2x_R - 1\right) \\ + \ln\left(\left(1 - x_R\right)/x_R\right)\end{matrix}\right] \quad (30)$$

with $E_{1/2} = E_a^o + \left(RT/nF\right)S\theta_T$ (31)

$$S = \left(a_{RR} - a_{OO}\right) \quad (32)$$

The parameter S defines the position of the peak on the potential axis. The peak potential, which occurs when $x_R = 0.5$, is equivalent to the half wave potential and therefore from Eq. (31) is a function of the fractional coverage.

Other workers have derived equations which have a final form very similar to those presented above [15-17]. The final equations derived by these authors are formally equivalent to the earlier derivation by Laviron.

When the reaction is no longer reversible the dimensionless current function is given by [18]

$$\psi = \xi\, dx_R / d\xi \quad (33)$$

where

$$\frac{dx_R}{d\xi} = -m\left\{\left(1-x_R\right)\xi^{-(1+\alpha)}\exp\left[-2\delta\theta_T + 2x_R\left(\delta-\gamma\right)\theta_T\right] - x_R\xi^{-\alpha}\exp\left[-2\zeta\theta_T + 2x_R\left(\zeta-\varphi\right)\theta_T\right]\right\} \quad (34)$$

where δ, γ, φ, and ζ are interaction coefficients. Equation (34) cannot be solve analytically but has been solved numerically for several values of the interaction coefficients. For irreversible reactions δ and γ on one hand and φ and ζ on the other hand exert their influence on the reaction separately. Consequently the cathodic and anodic peaks have a different shape but the shape is independent of m. As $m \rightarrow 0$ the reaction becomes irreversible. Changes in the magnitude of m serve to shift the peak along the potential axis as they did in the ideal case.

Matsuda et al. [19, 20] have pointed out that the derivation of the equations presented above assumes that a completely random distribution of molecules exists despite the presence of interactions. This is not self-consistent since the presence of interactions should give rise to some regularity. A more rigorous derivation of the effect of lateral interactions was therefore derived by Matsuda et al. [19, 20]. The equation for the peak was derived based on the assumption of irreversible adsorption of molecules in a two dimensional quasi-crystalline lattice. In the limiting case of the co-ordination number approaching infinity, i.e. a random distribution, Lavirons equations are obtained. Interestingly simulations of this model for non-random distributions showed that for $g\theta_T < -3$ two peaks will be observed for a one electron transfer with a minimum occurring midway between them.

The models discussed in this section focus exclusively on non-idealities caused by lateral interactions between adsorbates rely on finding values of interaction coefficients which produced good fits with experimental data. Unfortunately the interaction coefficients for a system have yet to be predicted based on the experimental conditions and the physical properties of the surface confined molecule in any quantitative way.

Effect of a Distribution of Formal Potentials

Models based on a distribution of formal potentials have been used as an explanation for peak broadening. Albery et al. [21] proposed a model in which each adsorbate has its own formal potentials and the values are distributed in a Gaussian distribution. The model was applied to explain the results for the reduction of a multilayer thionine coated electrode which did not fit the lateral interaction model given above. While in multilayers the formal potentials of each molecule are unlikely to be equivalent due to their different environments it is unclear whether a distribution of formal potentials within monolayers should be as significant. Nahir and Bowden [22] used a similar model to analyze the voltammograms of cytochrome *c* adsorbed on a self assembled monolayer (SAM). In this case differing orientations of the protein on the surface of the SAM may lead to an apparent distribution of formal potentials (Eq. 14).

The population of the *j*th species is normally distributed with the current being the sum of contributions from each of these species.

$$i = \sum_j p_j i_j \qquad (35)$$

The dimensionless current is given by

$$\psi = \sum_j p_j \frac{\xi_j}{\left(1+\xi_j\right)^2} \qquad (36)$$

which is analogous to Eq. (11) with ξ_j defined as

$$\xi_j = \exp\left[\left(\frac{nF}{RT}\right)E - E_j^o\right] \qquad (37)$$

and

$$p_j = \left(1/\sigma\sqrt{2\pi}\right)\exp\left[-\left(E_j^o\right)^2/2\sigma^2\right] \qquad (38)$$

where σ is the standard deviation in $E^o{}'$.

Effect of the Interfacial Potential Distribution

Both the models describing lateral interactions and also the more recent dispersion of formal potential models are essentially curve fitting exercises in the sense that fitting parameters are adjusted until a good agreement with experimental results is found. A physical meaning of what the magnitude of the various parameters might represent is at best fairly qualitative. The strength of the recent double layer models is that the input variables are usually known or can be readily measured independently allowing a calculation of the voltammetric peak and comparison with experimental results.

Smith and White [8] have recently derived an expression which assumes ideality but which takes into account the effect of the interfacial potential distribution (IPD). They assumed that the redox centers of the molecules are all distributed homogeneously in a plane, referred to as the plane of electron transfer (PET), at a finite distance, d_1, from the electrode (figure 1); that electrolyte ions from the solvent do not penetrate into the film; the diffuse capacitance is described by Gouy-Chapman theory; and that the dielectric permittivity of the adsorbed layer is constant. The dimensionless current is given by

$$\psi = \left(1 - \frac{\partial\phi_P}{\partial E}\right)\frac{\xi}{\left(1+\xi\right)^2} \qquad (39)$$

where ϕ_P is the potential difference between the plane of electron transfer and the bulk solution and ξ is given by

$$\xi = \exp\left[\left(\frac{nF}{RT}\right)E - \phi_P - E_a^o\right] \qquad (40)$$

When $\phi_P = 0$ Eqs. (39) and (40) reduce to those for the ideal case. Equation (39) can be rewritten as

$$\psi = \frac{\xi}{\left(1+\xi\right)^2}\frac{C_T}{C_1} \qquad (41)$$

where C_1 is the capacitance of the adsorbed layer $\left(C_1 = \varepsilon_0\varepsilon_1/d_1\right)$, ε_0 is the permittivity of free space, ε_1 is the dielectric constant of the adsorbed layer, d_1 is the thickness of the adsorbed layer, and C_T is the double layer capacitance given by Eq. (42)

$$C_T^{-1} = C_1^{-1} + \left(C_3^{-1} + C_2^{-1}\right)\left[1 + \left(n^2F^2\Gamma_T / RTC_1\right)x\right. \qquad (42)$$

In figure 1a the PET is assumed to lie at the interface between the surface bound molecule and solution therefore $C_2 = 0$. In figure 1b the PET is assumed to be buried within the SAM and C_2 is the capacitance of the layer between the PET and the solution given as

$$C_2 = \varepsilon_0\varepsilon_2/\left(d_2 - d_1\right) \qquad (43)$$

C_3 is the diffuse capacitance which for a symmetrical electrolyte is

$$C_3 = \varepsilon_o\varepsilon_3\kappa\cosh\left[zF\phi_2 / 2RT\right] \qquad (44)$$

ε_3 is the dielectric constant of the solvent, and κ is the inverse Debye length (for a symmetrical supporting electrolyte of charge z:z, $\kappa = zF\left(2000c_s / \varepsilon_o\varepsilon_3 RT\right)^{1/2}$ with c_S the molar concentration of the supporting

electrolyte, and ε_3 is the dielectric constant of the solvent).

The diffuse capacitance of a non-symmetrical electrolyte may be determined by taking the derivative of the equation for the diffuse charge, Eq. (45) [23, 24], with respect to ϕ_2 (or ϕ_P if it was assumed that the IPD was located at the monolayer-solution interface) [25].

$$\frac{(\sigma_3)^2}{\varepsilon_o \varepsilon_3 RT} = 2000 \sum c_i \left[\exp\left(-z_i F \phi_2 / RT\right) - 1 \right] \tag{45}$$

In extreme cases the existence of a potential difference between the PET and the bulk solution may lead to some distortion in the shape of the peak. This has been discussed in detail and examples were given by Smith and White [8]. Since no shift in peak potential with increasing sweep rate is predicted for reversible peaks affected by the IPD, experiments carried out at a range of sweep rates should enable one to distinguish between asymmetrical IPD distorted reversible peaks and those that are asymmetrical due to irreversible charge transfer. The peak potential and shape are effected by decreasing ionic strength and charge differences between Ox and Red, $z_O \neq z_R$. The effect on the peak potential can be quantified from Eq. (46)

$$\sigma_M + \sigma_P + \sigma_3 = 0 \tag{46}$$

where

$$\sigma_3 = \varepsilon_o \varepsilon_3 \kappa \sinh\left[zF\phi_P / 2RT \right] \tag{47}$$

when $d_2 - d_1 = 0$. We can use the relationship $\sinh^{-1}[u] = \ln\left[u + \left(u^2 + 1\right)^{1/2} \right]$ to show that ϕ_P depends on σ_P, i.e. surface coverage, and electrolyte concentration, according to

$$\phi_P \cong \left(2RT/zF\right) \ln \frac{\left(\sigma_M + \sigma_P\right)}{\left(2000 RT \varepsilon_0 \varepsilon_3\right)^{1/2}} - \left(2RT/zF\right) \ln\left(c_s\right)^{1/2} \tag{48}$$

From Eq. (48) we see that the peak potential, shifts by –59/z mV per ten fold increase in electrolyte concentration.

The capacitative current, $i_{cap} = \upsilon A C_T$, can be calculated from Eq. (42). According to the IPD model, for $z_O \neq z_R$, a capacitance minimum will occur at or near the peak potential. This is interesting because the usual method for integrating voltammetric peaks is to assume a linear baseline. It follows that in such cases where the IPD model is applicable estimations of peak area are likely to be understated if a linear baseline approximation is used. Smith and White have suggested that the background current may successfully be subtracted from the total current when $C_1^{-1} \gg C_3^{-1}\left[1 + \left(n^2 F^2 \Gamma_T / RTC_1\right) x_R \left(1 - x_R\right)\right]$ or when $i_f / i_{cap} \gg 1$ which occurs when $n^2 F^2 \Gamma_T d_1 / \varepsilon_0 \varepsilon_3 4RT \gg 1$.

Smith and White envisaged $d_2 - d_1 \neq 0$ only when the redox center is buried within the molecule. Fawcett [26] extended the work of Smith and White by including a Stern layer into the model. He pointed out that even when the redox center is located at the solution interface, a Stern layer, in which water molecules have a collectively different structure from the bulk, will exist (figure 2).

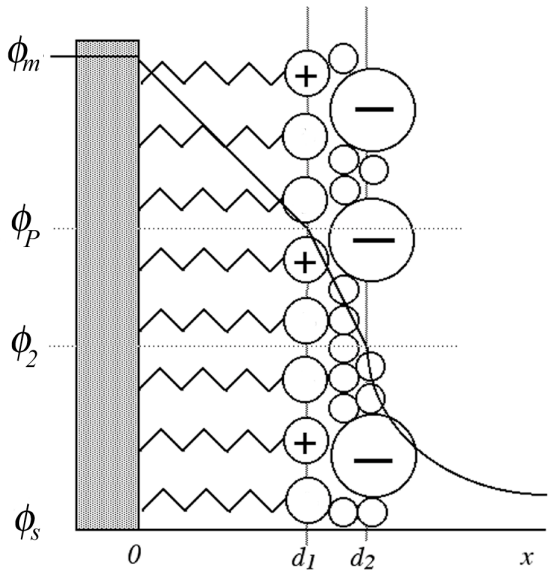

Figure 2. Same as figure 1a but with a Stern layer included which extends from d_1 to d_2. The potential profile in the region $d_1 \leq x \leq d_2$ which has a dielectric constant of ε_2 and capacitance C_2 is assumed to be linear.

It is assumed that the potential decays linearly within the Stern layer, which has a thickness and relative permittivity different from that of the monolayer and the bulk solution. In addition to allowing the inclusion of a Stern layer, Fawcett showed that to estimate the electrostatic potential of the ionized redox centers the variation in potential both parallel and perpendicular to the electrode solution interface must be considered. By allowing for discreteness-of-charge effects, which are important at phase boundaries where there is a sharp change in the dielectric property of the two media, the potential of the redox centers is defined as

$$\chi_P = \phi_P + \zeta \qquad (49)$$

where ζ is the discreteness of charge potential. Equations (39) to (44) can still be used for calculations providing χ_P is substituted for ϕ_P. Fawcett [26] determined ζ based on the cut-off disk model of Levine [27]. Levine's model assumes that the charge density on the inner Helmholtz plane (IHP) is considered to be uniform outside a disk surrounding the charged region of the molecule and that the radius of the cut off disk is much greater than the distance between the ionized redox centers and the electrode. When these assumptions are satisfied ζ is given by

$$(\xi)_{\text{cut-off disk}} = -\frac{b\sigma_P}{C_1 + C_2} \qquad (50)$$

where

$$b = \frac{C_3 + C_2}{C_3 + \left(C_1 C_2 / C_1 + C_2\right)} \qquad (51)$$

In sufficiently concentrated electrolyte solutions $b \rightarrow 1$. Since the cut-off disk model assumes that the thickness of the IHP is small relative to the distance between the redox centers themselves the calculations of ζ using this model are valid only at low adsorbate coverages.

Andreu et al. [28] used the hexagonal array model of Barlow and MacDonald for calculating ζ at higher coverages. In the hexagonal array model the redox centers are represented as point charges embedded in a dielectric medium of relative permittivity ε_1. The calculations required to arrive at a value for ζ are more complex than for the cut-off disk model and will not be discussed here but some general remarks about this model can be made. Calculations based on the hexagonal array model indicate that the cut-off disk model overcompensates for discreteness-of-charge effects at higher adsorbate coverages. The hexagonal array model is expected to fail when the redox adsorbates form molecular aggregates. Calculations of the IPD effects lie between those based on the IPD model with cut-off disk calculation of ζ and the IPD model of Smith and White. An important point to note is that for $d_2 \rightarrow 0$, $\zeta \rightarrow 0$ due to electrostatic screening of diffuse layer counter ions.

When the reaction is no longer reversible the equation for the dimensionless current is given by Eq. (16) and (17) with $\eta = E - \phi_P - E_a^r$ [12]. As $m \rightarrow 0$ the reaction becomes totally irreversible and for the cathodic curve $\eta^{1-\alpha} << \eta^{-\alpha}$ and $\eta << 1$ and for the anodic curve $\eta^{-\alpha} << \eta^{1-\alpha}$ and $\eta >> 1$. The peak potentials occur when [12]

$$\left(dx_R/dE\right)_{p_c} = -\left(1-x_R\right)_{p_c}\left(\alpha nF/RT\right)\left(1-d\phi_P/dE\right)_{p_c} \quad (52)$$

$$\left(dx_R/dE\right)_{p_a} = -\left(x_R\right)_{p_a}\left[\left(1-\alpha\right)nF/RT\right]\left(1-d\phi_P/dE\right)_{p_a} \quad (53)$$

where the subscript p refers to the value of the particular variable at the peak potential. Equating Eqs. (19) and (20) with Eq. (12) for $m \rightarrow 0$ gives the irreversible cathodic and anodic peak potentials

$$E_{p_c} = E_c^r + \phi_{p_c} - \frac{RT}{\alpha nF}\ln\left[\left(\alpha/m\right)\left(1-d\phi/dE\right)_{p_c}\right] \quad (54)$$

$$E_{p_a} = E_a^r + \phi_{p_a} - \frac{RT}{\left(1-\alpha\right)nF}\ln\left[\left(1-\alpha\right)\left(1-d\phi/dE\right)_{p_a}/m\right] \quad (55)$$

The rate constant for the reaction can be determined from the peak separation by subtracting Eq. (54) from (55) and rearranging to give

$$\ln k_s = \alpha\ln\left(1-\alpha\right) + \left(1-\alpha\right)\ln\alpha - \ln\left(RT/nF\left|\upsilon\right|\right) - \left[\alpha\left(1-\alpha\right)nF\Delta E_p / RT\right] + H \quad (56)$$

where H is a collection of terms

$$H = \alpha\left(1-\alpha\right)\left(nF/RT\right)\left(\phi_{p_a} - \phi_{p_c}\right) + \alpha\ln\left[1-\left(d\phi/dE\right)_{p_a}\right] + \left(1-\alpha\right)\ln\left[1-\left(d\phi/dE\right)_{p_c}\right] \quad (57)$$

which are due to the double layer effects.

Effect of Ion Pairing

Rowe and Creager [29] studied the effects of ion pairing on the peak potentials of adsorbed alkanethiol ferrocenes. After assuming that there is no ion pairing with the reduced form they showed that the peak potential shifts according to the following equation

$$E_p = E_p' - \left(RT/nF\right)\ln\left(1+\sum K_i c_i\right) \quad (58)$$

where E_p' is the peak potential in the absence of ion pairing, K_i is the equilibrium constant for ion pairing between Ox and the ith anion with bulk concentration c_i. With the exception of ion pairing the ideal case was assumed; however it would be relatively simple to extend the other models presented in this review to include ion pairing using this approach.

Ohtani et al. [30] have recently published a theory on the effect of ion pairing on linear sweep voltammograms which includes double layer effects analogous to those presented by Smith and White [8]. They allowed for both ion pairing and triple ion formation with the oxidized adsorbate.

$$O^+ + X^- \Leftrightarrow \left(OX\right)^0 \qquad K_{O1} \quad (59)$$

$$\left(OX\right)^0 + X^- \Leftrightarrow \left(OX_2\right)^- \quad K_{O2} \quad (60)$$

The dimensionless current was shown to be

$$\psi = \xi\Big/\left[\rho\left(1+\xi\right)^2 + M\xi\right] \quad (61)$$

where $\rho = \left(1 + \frac{C_1}{C_2} + \frac{\varepsilon_1}{\varepsilon_3\kappa d_1}\right)$ (62)

$$M = \left(z_O - z_R\right)\frac{F^2}{RT}\Gamma_T\left(\frac{1}{C_2} + \frac{1}{\varepsilon_3\varepsilon_0\kappa}\right) \quad (63)$$

$$\xi = K' \exp\left[\frac{F}{RT}\left(E_a^o - E_{pzc} - \frac{\sigma_M d_1}{\varepsilon_1 \varepsilon_0}\right)\right] \quad (64)$$

$$\text{and } K' = 1\Big/\left(1 + c_X K_{o1} + c_X^2 K_{o2}\right) \quad (65)$$

Ohtani et al. drew attention to the similarity of Eq. (61) with Eq. (26). If it is assumed that $\frac{C_1}{C_2} + \frac{\varepsilon_1}{\varepsilon_3 \kappa d_1} \to 0$, i.e. $\rho \to 1$, then both Eqs. (61) and (26) for the peak current, which occurs at x_R = 0.5 (ξ = 1), are identical if one sets $M = 2g\theta_T$. The authors explained that in a simple case where $z_R = 0$, z_O determines the polarity of g. The charge compensation of a cationic adsorbate by ion pairing is insufficient and therefore there is a net repulsion between cationic adsorbates. If a triple ion forms resulting in $z_O < 0$ the cationic adsorbate is stabilized by attractive forces. The peak potential is given by Eq (58).

$$E_p = \left[E_a^o + \left(RT/nF\right)\ln K'\right]\rho + \left(RT/nF\right)J \quad (66)$$

where

$$J = \frac{\left(z_O + z_R\right)n^2F^2\Gamma_T}{2RT}\left(\frac{1}{C_2} + \frac{1}{\varepsilon_3\varepsilon_0\kappa}\right) \quad (67)$$

Following the same argument as above Eq (66) is identical in form to Eq. (31) if one sets $J = S\theta_T$. Simulated voltammograms showed that as a result of ion pair formation peaks were smaller and broader than for the ideal case. When triple ion formation occurred the peaks were sharper and narrower than ideal.

Andreu et al. [31] considered ion pairing between electrolyte ions and both the oxidized and reduced molecule. Their calculations indicated that when the redox centre is at the end of the molecule (figure 1a) the dependence of the peak potential on bulk concentration of the ion X^- is

$$E_p = E_a^o + \frac{RT}{nF}\ln\frac{\prod_{i=1}^{|z_R|} K_{R,i}}{\prod_{i=1}^{|z_O|} K_{O,i}} - \frac{\left|z_O\right| - \left|z_R\right|RT}{nF}\ln c_x \quad (68)$$

Equations (48), and (66) to (68) indicate that it may be difficult to distinguish between peak shifts due to ion pairing and those due to double layer effects. For this reason it is important that the ionic strength is kept constant when quantities of an electrolyte suspected of forming ion pairs is added to the solution.

Effect of Acid-Base Equilibria

Smith and White have derived an expression which assumes ideality but which takes into account the effect of the acid-base dissociation of the molecule at the plane of acid dissociation (PAD) [32]. The proton from the surface bound molecule is assumed to be in equilibrium with the protons in the bulk solution.

$$HA \Leftrightarrow H^+ + A^- \quad (69)$$

$$\log\left[x_A/\left(1 - x_A\right)\right] = pH - pK_a + \left(F\phi_{PAD}/2.3RT\right) \quad (70)$$

The capacitance is given by Eq. (71)

$$C_T^{-1} = C_1^{-1} + \left(C_3 + C_{HA}\right)^{-1} \quad (71)$$

$$\text{where } C_{HA} = \left(F^2\Gamma_T/RT\right)x_A\left(1 - x_A\right) \quad (72)$$

is the capacitance due to the acid-base dissociation. This model has been further refined by Fawcett and co-workers [33, 34] by taking into account the "discreteness of charge" effect. Using the cut-off disk model the equation for the capacitance is [33]

$$\frac{1}{C_T} = \frac{1}{C_3} + \frac{C_1 + C_2}{C_1C_2} - \left(\frac{C_{HA}}{C_3} + \frac{C_{HA}}{C_2}\right)\frac{d\chi}{d\sigma_M} \quad (73)$$

$$\chi = \phi_{PAD} + \zeta \quad (74)$$

Simulations based on this model produce results which are markedly

different from that of Smith and White's model. The assumptions made in the cut-off-disk model implies that this model is best suited for adsorbed layers with only a small amount of ionizable adsorbate. For higher coverages another model was proposed by Andreu and Fawcett [34] based on the hexagonal array model of Barlow and MacDonald [35]. Relatively good agreement was found between experiment results and those predicted by the hexagonal array model.

Ideal Case incorporating Marcus Theory

The discussions so far have been based on Butler-Volmer kinetics in which the overpotential is assumed to be much smaller than the solvent reorganization energy of the reaction. The development of self assembled monolayers in which an electroactive center could be positioned at fixed distances from the electrode has opened up the study of electrochemical reactions which can be used to test Marcus theory [36]. The initial use of Marcus theory in an experimental model was for chronoamperometry [37] but recently theories for LSV and CV have been published [11, 38]. One of the interesting features of this model is that it predicts that the rate constant should reach a constant maximum value at high η. A decrease in the rate at high η, which is seen for homogeneous reactions (the Marcus inverted region) is absent for heterogeneous electron transfer due to the continuum of electronic states in the metal electrode [37]. The rate constant for cathodic and anodic reaction in which their is weak electronic coupling between the reactants is [37]

$$k_{f,b} = k_{\max}\left(\frac{RT}{4\pi N_A \lambda}\right)^{1/2} \int_{-\infty}^{\infty} \frac{1}{1+\exp(x)} \exp\left\{-\left[\frac{N_A\lambda \pm F\eta}{RT} - x\right]^2 \frac{RT}{4N_A\lambda}\right\} dx \quad (75)$$

where N_A is Avogadro's number, λ is the reorganization energy in electron Volts, x is a dimensionless integration variable, and $k_{\max}$ is the maximum value of the rate constant given by

$$k_{\max} = \frac{4\pi^2 \rho H_{AB}^2}{h} \quad (76)$$

In Eq. (76) ρ is the density of electronic states in the metal which is assumed to be independent of electrode potential, h is Planck's constant and H_{AB} is the electronic coupling matrix element which describes the electronic coupling of reactants electronic state with the products. For this discussion it is assumed that for a non-adiabatic electron transfer the electronic coupling is < 50 cm^{-1} (0.6 kJ mol^{-1}). The magnitude of $k_{\max}$ shows an exponential distance dependency given by

$$k_{\max} \propto \exp\left[-\beta\left(d - d_o\right)\right] \quad (77)$$

where d_o is the minimum redox center to electrode distance, and β is a decay constant which depends on the structure through which the tunneling occurs. For self assembled monolayers of the alkanethiol type on gold electrodes β is frequently found to be ~ 1.1 $Å^{-1}$ per methylene group [4]. The standard rate constant can be determined from Eq. (75) by setting $\eta = 0$.

$$k_s = k_{\max}\left(\frac{RT}{4\pi N_A \lambda}\right)^{1/2} \int_{-\infty}^{\infty} \frac{1}{1+\exp(x)} \exp\left\{-\left[\frac{N_A\lambda}{RT} - x\right]^2 \frac{RT}{4N_A\lambda}\right\} dx \quad (78)$$

Equations (75) and (2) cannot be solved analytically but an analytical approximation is available [11]. Information on the factors influencing the shape and position of the peaks have been gained from numerical simulations [11]. As expected, voltammetric peaks that were calculated from Eqs. (75), (78) and (2) were identical to those calculated from Eq. (18) for $\lambda \rightarrow \infty$ i.e. when the current-potential equation reduces to the Butler-Volmer equation [11, 38]. While Lavirons theory, based on Butler-Volmer kinetics predicts that the irreversible peak shape should be a constant asymmetric shape, the model based on Marcus theory predicts the peak shape to be dependent on λ and the peak shape should change with increasing sweep rate. This is a key difference between the two models.

As the sweep rate is increased peaks become progressively broader and flatter and at sufficiently high values of $F\eta/\lambda$ the peaks show diffusional type tailing and eventually the determination of E_p becomes difficult. For small to moderate overpotentials the value of k_s obtained from ΔE_p does not deviate much from that predicted by Butler-Volmer kinetics. On the other hand the peak current is greatly dependent on λ. Numerical simulations assume or require that all the redox centers have the same rate of reaction with the electrode. A dispersion in the rate of the reaction can be inferred from non-linearity of log (i) versus time plots from chronoamperometry experiments.

One of the suggested causes for apparent non-ideal voltammograms has been kinetic dispersion. This phenomena is closely linked to the distribution of formal potentials discussed above. Equation (75) shows that any dispersion of formal potentials will lead to an *apparent* dispersion in electron transfer rates. Distribution of formal potentials is indicated by peak broadening of reversible voltammograms provided that other causes of peak broadening can be ruled out. Some of the phenomena that may cause *real* kinetic dispersion are

(a) a variation of the dipolar environments around redox sites leading to a dispersion in λ;

(b) a dispersion of tunneling distance, d;

(c) a dispersion in the coupling term, β, caused by conformational changes within the monolayer structure.

Effect of Uncompensated Resistance

The most likely source of the reversible peak splitting may be the effects of uncompensated resistance. The work of Ravenscroft and Finklea [39] is noteworthy because when the uncompensated resistance was reduced to around 4 Ω the CVs were ideal within experimental error. The effects of uncompensated resistance have been discussed by Roullier and Laviron [40]. The current is given by the differential equation

$$\frac{di}{dt} = R_u^{-1}\left[1 - \frac{RTi\left(1+\xi\right)^2}{n^2F^2AR_u\Gamma_T}\right] \qquad (79)$$

where R_u is the uncompensated resistance and

$$\xi = \exp\left[\left(\frac{nF}{RT}\right)E - E_a^o - iR_u\right] \qquad (80)$$

The effects of uncompensated resistance are such that it is impossible to distinguish them with slow kinetics which suggests that rate constants determined by Eq. (21) are likely to be under estimated.

References

1. E. Laviron, "Voltammetric Methods for the Study of Adsorbed Species", in A. J. Bard (Ed.), *Electroanalytical Chemistry,*

Vol. 12, Marcel Dekker, New York, 1982, p. 53
2. R. W. Murray, "Chemically Modified Electrodes", in A. J. Bard (Ed.), *Electroanalytical Chemistry, Vol. 13*, Marcel Dekker, New York, 1982, p. 191
3. R. W. Murray, "Introduction to the Chemistry of Molecularly Designed Electrode Surfaces", in R. W. Murray (Ed.), *Molecular Design of Electrode Surfaces,* John Wiley & Sons, New York, 1992, p. 1
4. H. Finklea, "Electrochemistry of Organised Monolayers of Thiols and Related Molecules on Electrodes", in A. J. Bard, I. Rubenstein (Ed.), *Electroanalytical Chemistry, Vol. 19*, Marcel Dekker, New York, 1996, p. 110
5. M. J. Honeychurch and G. A. Rechnitz, *Electroanalysis*, **10** (1998) 285
6. M. J. Honeychurch and G. A. Rechnitz, *Electroanalysis*, **10** (1998) 453
7. E. Laviron, *J. Electroanal. Chem.*, **100** (1979) 263
8. C. P. Smith and H. S. White, *Anal. Chem.*, **64** (1992) 2398
9. G. K. Rowe and S. E. Creager, *J. Phys. Chem.*, **98** (1994) 5500
10. E. Laviron, *J. Electroanal. Chem.*, **101** (1979) 19
11. M. J. Honeychurch, *Langmuir*, **15** (1999) 5158
12. M. J. Honeychurch, *Langmuir*, **14** (1998) 6291
13. E. Laviron, *J. Electroanal. Chem.*, **52** (1974) 395
14. E. Laviron, *J. Electroanal. Chem.*, **63** (1975) 245
15. D. F. Smith, K. Willman, K. Kuo and R. W. Murray, *J. Electroanal. Chem.*, **95** (1979) 217
16. A. P. Brown and F. C. Anson, *Anal. Chem.*, **49** (1977) 1589
17. K. Kano and B. Uno, *Anal. Chem.*, **65** (1993) 1088
18. E. Laviron and L. Roullier, *J. Electroanal. Chem.*, **115** (1980) 65
19. H. Matsuda, K. Aoki and K. Tokuda, *J. Electroanal. Chem.*, **217** (1987) 1
20. H. Matsuda, K. Aoki and K. Tokuda, *J. Electroanal. Chem.*, **217** (1987) 15
21. W. J. Albery, M. G. Boutelle, P. J. Colby and A. R. Hillman, *J. Electroanal. Chem.*, (1982) 135
22. T. M. Nahir and E. F. Bowden, *J. Electroanal. Chem.*, **410** (1996) 9
23. R. J. Hunter, "*Foundations of Colloid Science Vol. 1*", Oxford University Press, Oxford, 1987, p.386
24. K. B. Oldham, *J. Electroanal. Chem.*, **63** (1975) 139
25. M. J. Honeychurch, *J. Electroanal. Chem.*, **445** (1998) 63
26. W. R. Fawcett, *J. Electroanal. Chem.*, **378** (1994) 117
27. S. Levine, *J. Colloid Interface. Sci.*, **37** (1971) 619
28. R. Andreu, J. J. Calvente, W. R. Fawcett and M. Molero, *Langmuir*, **13** (1997) 5189
29. G. K. Rowe and S. E. Creager, *Langmuir*, **7** (1991) 2307
30. M. Ohtani, S. Kuwabata and H. Yoneyama, *Anal. Chem.*, **69** (1997) 1045
31. R. Andreu, J. J. Calvente, W. R. Fawcett and M. Molero, *J. Phys. Chem. B*, **101** (1997) 2884
32. C. P. Smith and H. S. White, *Langmuir*, **9** (1993) 1
33. W. R. Fawcett, M. Fedurco and Z. Kovacova, *Langmuir*, **10** (1994) 2403
34. R. Andreu and W. R. Fawcett, *J. Phys. Chem.*, **98** (1994) 12753
35. C. A. Barlow and J. R. MacDonald, "Theory of Discreteness of Charge Effects in the Electrolyte Compact Double Layer", in P. Delahay (Ed.), *Advances in Electrochemistry and Electrochemical Engineering, Vol. 6*, John Wiley & Sons, New York, 1967, p. 1

36. V. G. Levich, "Kinetics of Reactions with Charge Transport", in H. Eyring (Ed.), *Physical Chemistry; an Advanced Treatise, Vol. 9B*, Academic Press, New York, 1970, p. 985
37. C. D. Chidsey, *Science*, **251** (1991) 919
38. K. Weber and S. E. Creager, *Anal. Chem.*, **66** (1994) 3164
39. M. S. Ravenscroft and H. O. Finklea, *J. Phys. Chem.*, **98** (1994) 3843
40. L. Roullier and E. Laviron, *J. Electroanal. Chem.*, **157** (1983) 193